LABORATORY SIMULATION OF LARGE SCALE FRAGMENTATION

Robert M. Schmidt and Kevin R. Housen
Boeing Aerospace & Electronics, M/S 3H-29, Seattle WA 98124

Housen and Holsapple (1990) have advocated that self compression of large bodies due to gravity can be simulated by applying external pressure. To evaluate this simulation technique, a 13-inch diameter cylindrical test chamber with L/D of 1 has been fabricated to accommodate firing explosive charges with gas overpressures of up to 6000 psi. The chamber can be used with liquids up to 9000 psi. A primary objective was to investigate a weakly cemented basalt that has been developed as a simulant for jointed basalt in subscale cratering investigations. This material is comprised of 50% basalt 2-mm aggregate, 20% 0.4-mm iron grit, 22% type F flyash, 2% type C flyash, and 6% water. The material bulk density is 2.6 gm/cc, the static unconfined compressive strength is 101 ± 33 psi and the static tensile strength (ASTM 496) is 17.2 ±0.94 psi. These strengths are averages based on 22 compression tests and 8 tension tests for cure times of 7 to 42 days corresponding to specific target ages.

Samples were cast in 15 cm diameter spherical molds and allowed to cure for at least 7 days. Standard cylindrical specimens were also cast to be used in strength measurements at the time the spheres were used. An explosive charge was grouted into each sample. Although the equivalent charge burial depth to simulate impact fragmentation has not yet been established, a depth of approximately 1 charge radius was used, as suggested by Holsapple (1980) for impact cratering. Variations in the burial depth over the range of 1 to 2 charge radii did not seem to produce significant differences. However, some calibration experiments should be performed to verify this. A single impact test was conducted (shot 876), but was of insufficient energy to produce a useful evaluation of equivalence.

A baseline fragmentation curve for ambient one atmosphere conditions (zero overpressure) is shown in Fig. 1, which is a plot of the ratio of the mass of largest fragment divided by the target mass versus the explosive energy divided by the target mass. Also shown are the data points and projected curves for the nine different overpressures tested (see Housen, *et al.*, 1991). These data show that the fragmentation strength increases by a factor of 20 to 40 over the range of pressures tested. An important observation was that for pressurized targets as much as 50% of the target could be cratered leaving the other half intact as a single fragment.

A second target material was supplied by D. R. Davis and E. V. Ryan of Planetary Science Institute in Tucson. This material is a cement and sand mortar that has been tested extensively in impact experiments using the AVGR as described by Davis and Ryan (1990). Two separate batches were supplied, each accompanied with two cylindrical test specimens which were tested to characterize the unconfined compression and tensile strength for these targets. The first batch consisted of three freshly made 10.7-cm diameter weak cement mortar spheres, dyed yellow. Two unconfined compression test cylinders provided strengths of 414 and 452 psi. Also included were two older spheres of the same size, dyed pink: one of weak mortar (18 months old with estimated compressive strength of 500 psi) and one intermediate strength mortar sphere (5 years old with estimated strength of 3000 psi). The second batch consisted of six freshly made 10.7-cm spheres, white in color. The three yellow spheres were used to define an ambient one atmosphere fragmentation curve as shown in Fig. 2. The weak pink sphere (shot 872) was then used to establish the existence of a pressure effect for this material. Subsequent tests with the white spheres produced a self-consistent pressure strengthening effect with the exception of shot 883 tested at 3000 psi. The target appeared to have only cratered in a manner expected for this pressure, however when the sample was picked up for weighing, it disintegrated into very small pieces. To test if the material had perhaps failed statically due to the overpressure loading, a second white sphere was subjected to the same 3000psi overpressure and then drilled and tested at one atmosphere (shot 884). It compared favorably with shot 872, which was fired with the same charge mass at one atmosphere, indicating that a static failure did not occur. A final test (shot 886) was made with the pink intermediate strength old sphere to investigate this anomaly. Taking an estimated tensile strength of 600 psi into account, it is consistent with expectations as seen in Fig. 2. Additional shots with the weak mortar are planned to fill in this gap in the data.

All materials tested show significant pressure strengthening. Relating these results to self gravity and scaling implications are discussed in a companion abstract by Housen, K. R. *et al.* (1991).

Davis, D. R. and E. V. Ryan (1990) Collisional disruption experiments, *Icarus 83*, 156-182.

Holsapple, K. A. (1980) Equivalent depth of burst for impact cratering, *Proc. LPSC 11th*, 2379-2401.

Housen, K. R. and K. A. Holsapple (1990) Fragmentation of asteroids, *Icarus 84*, 226-253.

Housen, K. R. *et al.* (1991) Scaling of fragmentation, *LPS XXII*, this volume.

# shot number	# sample number	c comp strength	t tensile strength	Qex specific energy	m expl mass	P over press	delta expl density	dob burial depth	d/a depth/ radius	M target mass	rho target density	R target radius	ML largest fragmen	Q collision energy/ target mass	ML/M frag/ total
-	-	(psi)	(psi)	(ergs/gm)	(gm)	(psi)	(gm/cc)	(cm)	-	(gm)	(gm/cc)	(cm)	(gm)	-	-
876	wcb 11	127	16.7	2.12E+10	0.37	0	2.79	impact		4556	2.71	7.38	4183	1.7E+06	0.92
863	wcb 1	101	*15.3*	4.25E+10	0.49	0	1.45	1.07	2.48	4232	2.66	7.24	3153	4.9E+06	0.75
867	wcb 4	60	*12.9*	4.25E+10	1.5	0	1.45	0.85	1.35	4347	2.64	7.33	715	1.5E+07	0.16
875	wcb 10	118	17.5	3.85E+10	4	0	1.48	1.19	1.38	4512	2.69	7.37	202	3.4E+07	0.04
877	wcb 12	143	17.2	3.85E+10	4	30	1.48	1.42	1.64	4486	2.67	7.37	1621	3.4E+07	0.36
880	wcb 14	108	15.9	3.85E+10	8	45	1.48	0.97	0.89	4583	2.73	7.37	258	6.7E+07	0.06
878	wcb 13	121	16.6	3.85E+10	4	75	1.48	1.37	1.59	4562	2.72	7.37	2968	3.4E+07	0.65
874	wcb 9	121	17.5	3.85E+10	4	90	1.48	1.42	1.64	4427	2.64	7.37	3086	3.5E+07	0.70
873	wcb 8	88	*14.6*	3.85E+10	16	370	1.48	1.64	1.20	4347	2.59	7.37	2338	1.4E+08	0.54
871	wcb 6	88	*14.6*	4.25E+10	8	750	1.45	1.88	1.72	4329	2.59	7.36	3617	7.9E+07	0.84
870	wcb 7	84	*14.4*	4.25E+10	4	1000	1.45	1.22	1.40	4346	2.60	7.36	4114	3.9E+07	0.95
868	wcb 5	60	*12.9*	4.25E+10	1.5	3000	1.45	0.56	0.89	4415	2.64	7.36	4320	1.4E+07	0.98
869	wcb 3	87	*14.6*	4.25E+10	1.5	3000	1.45	0.56	0.89	4231	2.64	7.26	4160	1.5E+07	0.98
864	wm 1y	*433*	*49.3*	4.25E+10	0.25	0	1.45	0.53	1.54	1074	1.77	5.25	911.4	9.9E+06	0.85
884	wm 26w	*573*	*51.7*	4.25E+10	0.49	0	1.45	0.53	1.23	1042	1.72	5.25	502	2.0E+07	0.48
866	wm 3y	*433*	*51.7*	4.25E+10	0.49	0	1.45	0.53	1.23	1125	1.86	5.25	892.3	1.9E+07	0.79
865	wm 2y	*433*	*49.3*	4.25E+10	1	0	1.45	1.02	1.86	1042	1.72	5.25	256.8	4.1E+07	0.25
879	wm 21w	*573*	*65.3*	3.85E+10	8	450	1.48	0.965	0.89	1007	1.66	5.25	7.2	3.1E+08	0.01
881	wm 22w	*573*	*65.3*	3.85E+10	8	450	1.48	0.965	0.89	1049	1.73	5.25	10	2.9E+08	0.01
872	wm 13p	*433*	*49.3*	4.25E+10	1	750	1.45	0.87	1.59	980	1.63	5.24	871.5	4.3E+07	0.89
885	wm 23w	*573*	*65.3*	3.85E+10	2	750	1.48	0.608	0.89	1008	1.66	5.25	841	7.6E+07	0.83
882	wm 24w	*573*	*65.3*	3.85E+10	4	750	1.48	0.876	1.01	1018	1.68	5.25	69	1.5E+08	0.07
883	wm 25w	*573*	*65.3*	3.85E+10	4	3000	1.48	0.86	1.00	1009	1.67	5.24	38	1.5E+08	0.04
886	ism 4g	*3000*	*341.9*	3.85E+10	4	3000	1.48	0.84	0.97	1225	2.02	5.25	1176	1.3E+08	0.96

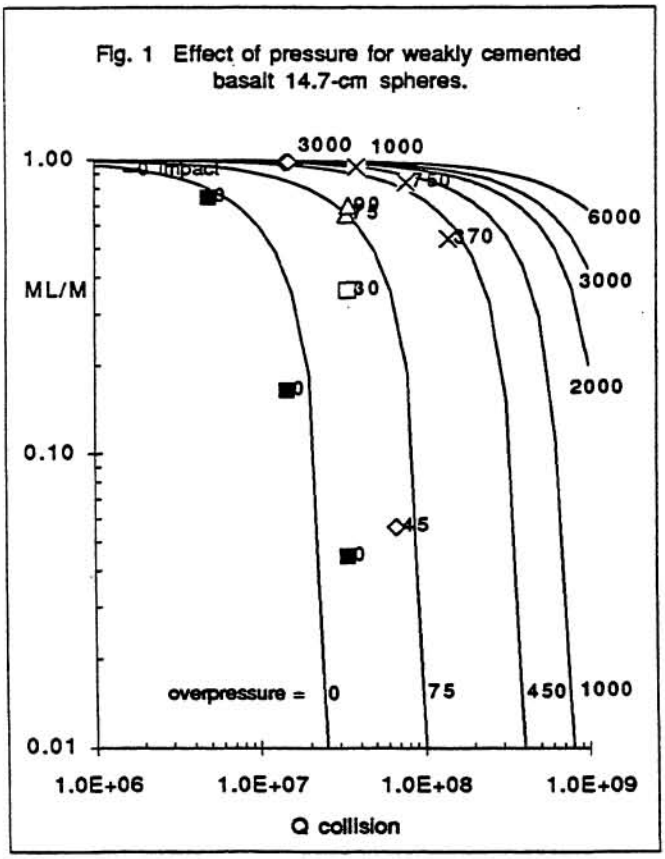

Fig. 1 Effect of pressure for weakly cemented basalt 14.7-cm spheres.

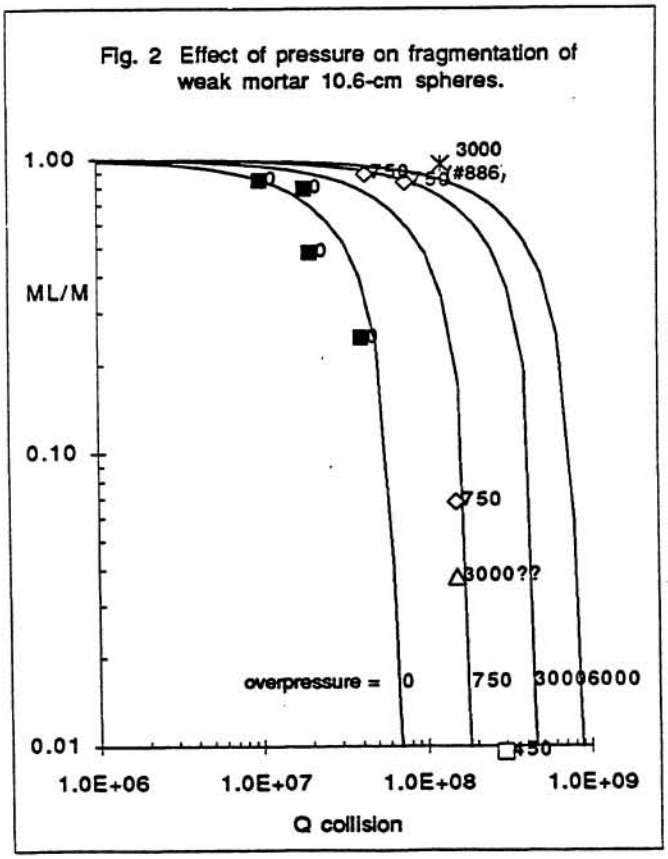

Fig. 2 Effect of pressure on fragmentation of weak mortar 10.6-cm spheres.